Applied Geochemistry 102 (2019) 88–101

Contents lists available at ScienceDirect

Applied Geochemistry

journal homepage: www.elsevier.com/locate/apgeochem

Geochemical and hydrological controls of arsenic concentrations across the sediment–water interface at Maharlu Lake, Southern Iran

R. Khosravi[a], M. Zarei[a,*], O. Sracek[b], M. Bigalke[c]

[a] Department of Earth Sciences, Faculty of Science, Shiraz University, Shiraz, Iran
[b] Department of Geology, Faculty of Science, Palacký University, 17. Listopadu 12, 771 46, Olomouc, Czech Republic
[c] Institute of Geography, University of Bern, Hallerstrasse 12, 3012, Bern, Switzerland

ARTICLE INFO

Editorial handling by Huaming Guo

Keywords:
Arsenic
Sediment–water interface
Hypersaline lake
Pore water
Surface water

ABSTRACT

The sediment–water transition zone in an aquatic system is key role to the distribution of contaminants between the surface water and sediment pore water. Maharlu Lake is a seasonal hypersaline lake in the central part of the Maharlu Basin in Southern Iran. Wastewater of various types produced within the basin is released into the seasonal freshwater rivers that ultimately drain into the lake. Samples were collected through one complete period of the lake water-level fluctuation. Lake surface water and shallow sediment pore water samples were collected three times at three piezometric stations at different distances from the river inflow points. Lake sediment samples were collected twice, and water samples from the inflowing rivers were collected five times. Changes in surface runoff and agricultural wastewater inflows were responsible for seasonal hydrochemical changes and changes in the As concentrations in the inflowing rivers. Data from the stations close to the river inflows indicated that the dissolved As concentrations across the sediment–water interface in Maharlu Lake are mostly controlled by evaporation and interactions between the surface water and shallow pore water. However, data from the station far from the freshwater inflows indicated that the brine and precipitated evaporites were at equilibrium and redox processes (e.g., iron (hydr)oxide dissolution and secondary sulphide precipitation) control the dissolved As concentration in pore water. The results confirmed the role of lake water evaporation in As enrichment and As sequestration by secondary sulphide minerals in sediment below the sediment–water interface. Climate change may alter the lake chemistry and As behavior in near future.

1. Introduction

The sediment–water interface (SWI) or pore water (PW)/surface water (SW) transition zone in an aquatic system plays a key role in controlling contaminant exchange between lake water and groundwater (Ford et al., 2005). Maharlu Lake is a seasonal hypersaline lake southeast of Shiraz City in the central part of the Maharlu Basin in southern Iran (Fig. 1). Maharlu Lake receives all surface flows from the basin. Migratory birds visit the lake, and halite is harvested from it for industrial and household use. Rapid urban and industrial development has continued without appropriate environmental planning in the northwestern part of the Maharlu Basin in recent decades, and this has caused the pollutant loads of the rivers (such as the Babahaji River (BR) and Khoshk River (KR)) that drain into Maharlu Lake to increase (Qishlaqi et al., 2008). A map of the Maharlu Basin is shown in Fig. 1. The rivers flowing into Maharlu Lake are now polluted or have critical concentrations of B, Pb, Sb, and Se (Najmodini, 2011).

The Surface sediment in Maharlu Lake is contaminated with heavy metals, and the pollutant concentrations are higher near the river inflow points than elsewhere (Moore et al., 2009). However, As in Maharlu Lake has a low enrichment factor (3.5), a low geoaccumulation index (≤ 0), and a low contamination factor (0.9), implying that it mainly has natural sources here (Moore et al., 2009). The As concentrations are several times higher in the lake SW (mean 187 $\mu g\,L^{-1}$) than in the inflowing river water ($\leq 5\ \mu g\,L^{-1}$), and the concentration in the SW increases with distance from the river inflow points (Najmodini, 2011). The water quality in the aquifers adjacent to Maharlu Lake is deteriorating because of intrusions of brine from the lake, and the As concentrations in the aquifers are also increasing (Bahmani, 2009).

The behavior of As in aquatic systems has been studied intensively because of the potential toxicity of As to organisms, including humans. The mobility and toxicity of As, and changes in As speciation caused by varying redox conditions in saline and freshwater lakes, ponds, and streams have been reported previously (Brandenberger et al., 2004;

* Corresponding author.
E-mail address: zareim@shirazu.ac.ir (M. Zarei).

https://doi.org/10.1016/j.apgeochem.2019.01.008
Received 1 April 2018; Received in revised form 9 December 2018; Accepted 19 January 2019
Available online 24 January 2019
0883-2927/

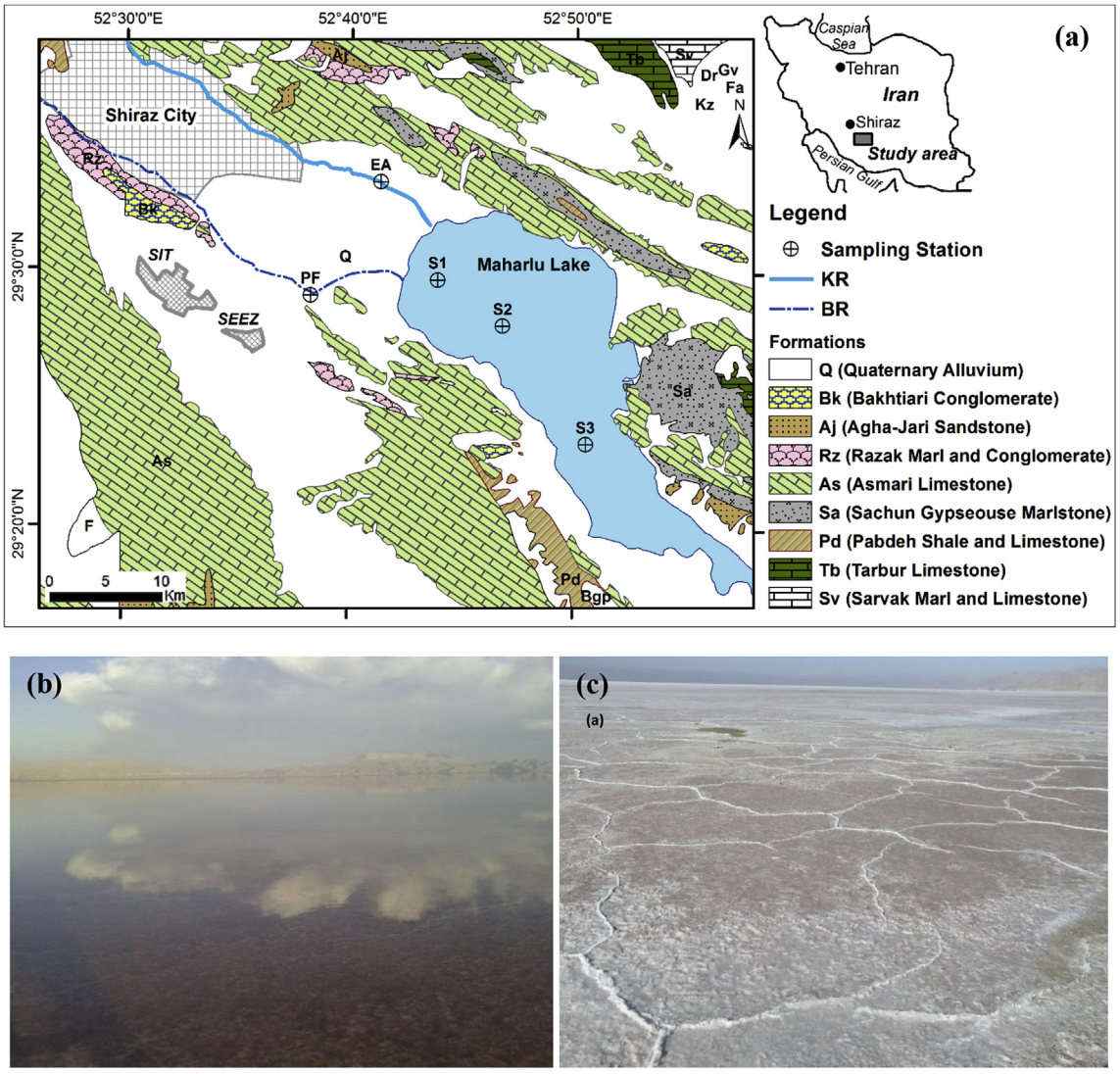

Fig. 1. (a) Geological map of the study area (modified from a 1:250000 map of Shiraz, National Iranian Oil Company, second edition, 1979). SIT and SEEZ are the Shiraz Industrial Town and Shiraz Especial Economic Zone, respectively, which release wastewater into the Babahaji River. PF and EA are the sampling stations on the Babahaji River and Khoshk River, respectively. The surface water and sediment pore water sampling stations along the longitudinal axes of Maharlu Lake are marked S1, S2, and S3. Subfigures (b) and (c) are photographs of Maharlu Lake in the wet and dry seasons, respectively.

Deng et al., 2014; Ford et al., 2005; Hollibaugh et al., 2005; Martin and Pedersen, 2002; Ryu et al., 2002; Du Laign et al., 2009; Langner et al., 2012). The sources of As, hydrochemical water type, pH, redox conditions, and degree of evaporation have been found to be principal factors controlling As concentrations, mobility, and toxicity in lakes. Sulphides, iron and manganese oxyhydroxides, and particularly organic matter play important roles in controlling As mobility in stream, lake, and wetland sediment (Galloway et al., 2018; Langner et al., 2014; Lawson et al., 2016; Neubauer et al., 2013).

We have previously studied spatial and seasonal variations in the chemical compositions of SW and PW in Maharlu Lake (unpublished data). The results indicated that the SW and PW chemical compositions are mainly controlled by evaporative evolution of the brine, dissolution/precipitation of evaporites, and diagenetic evolution of secondary carbonates. In a detailed study of hydraulic and hydrochemical interactions between the SW and PW across the SWI in Maharlu Lake we found a general downward flow from the SW to the PW at the bottom of the lake (unpublished data). The maximum downward flow rate (about 1 m y^{-1}) was found close to the river inflow area. Vertical flow across the SWI far from the river inflow area is limited due to an impermeable layer reducing hydraulic connectivity between the SW and shallow PW.

The aims of the study presented here were to investigate and interpret:

1) seasonal As concentration variations in the rivers flowing into Maharlu Lake using hydrological and hydrochemical data;
2) the As concentration distributions in the SW, PW, and shallow lake sediment; and
3) the overall behavior of As in the lake in response to the SW and PW chemical compositions and hydrological processes, including lake water level (LWL) fluctuations, evaporation, and SW–PW mixing across the SWI, taking into account the distance from inflowing rivers and depth.

2. Material and methods

2.1. Study area

The Maharlu Lake has an area of about 230 km^2 and an average elevation of 1425 m above sea level, and lies in the closed Maharlu Basin in southern Iran. Long-term climatological data (for 50 y) from the nearest climatological station to the lake (Dobaneh Climatological

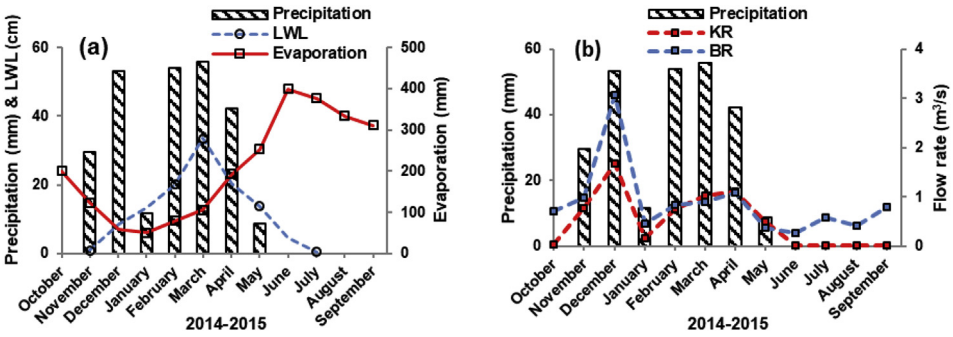

Fig. 2. (a) Monthly precipitation and (pan) evaporation (measured at the Dobaneh Climatological Station) and the measured lake water level (LWL). The sampling dates are marked with open circles on the LWL curve. (b) Babahaji River (BR) and Khoshk River (KR) flow rates at the hydrometric stations marked PF and EG in Fig. 1 and precipitation from October 2014 to September 2015 (Khosravi et al., 2018).

Station) indicate that mean annual precipitation is 341 mm and that potential mean annual evaporation is about seven times higher, at 2572 mm. The mean annual minimum and maximum temperatures are 9.0 and 25.2 °C, respectively. Most geological formations in the Maharlu Basin are composed of carbonates, conglomerates, evaporites, marl, sandstone, and shale formed in the Mesozoic and the Cenozoic (Fig. 1).

Maharlu Lake is a seasonal playa lake, and the LWL is mostly controlled by precipitation and evaporation (Fig. 1a Khosravi et al. (2018)). The LWL increases in the wet season with precipitation before decreasing in the dry season until the lake completely dries out because of the lack of precipitation and high evaporation rate (Fig. 2a; Khosravi et al. (2018)). The KR and BR are ephemeral rivers enter Maharlu Lake from the west (Fig. 1a). Their flow rates are controlled by seasonal precipitation and surface runoff in the study area (Fig. 2b), and both rivers receive untreated urban, industrial, and agricultural wastewater discharges, discharging directly into Maharlu Lake. There are no reliable estimates of total wastewater volumes released into the KR and BR or of the proportions of wastewater discharged by different sources. Building materials, electronic production facilities, a municipal landfill, paint factories, and untreated urban wastewater may be anthropogenic sources of heavy metals in the Maharlu Lake watershed (Moore et al., 2009).

A thick evaporite stratum has accumulated on the bed of Maharlu Lake because of intensive evaporation (Shariati Bidar, 2001). A pure halite layer 0–60 cm thick covers the lake and is extracted for industrial and household use. Field observations have shown that there is a sequence of unconsolidated sediments to about 1 m deep below the halite crust.

This sequence is composed of black organic-rich material, a green–gray zone composed of sulphates, halite, and carbonates, and sticky brown sediment composed mostly of aluminosilicates, carbonates, sulphates, and halite (Khosravi, 2018). The sediment porosity ranges from 28% to 40% and the grain sizes range from clay to silt (Khosravi, 2018).

Flow across the SWI in Maharlu Lake is generally downwards all year round (unpublished data). The leakage rate decreases as the distance from river inflows increases. Vertical flow is limited by a poorly permeable layer 50–100 cm deep in areas far from the river inflows (site S3). This layer creates semi-confined conditions below 100 cm deep with a high hydraulic head and a different PW chemistry from higher levels (unpublished data).

2.2. Sampling

The geochemical and hydrological factors controlling As distribution across the SWI in Maharlu Lake were investigated by collecting and analysing samples of inflowing river water, lake SW, shallow lake sediment PW, and shallow lake sediment. The sampling times were determined by LWL fluctuations and are marked with open circles on the LWL curve in Fig. 2a. The SW and PW samples were collected 1) before freshwater entered the lake in November 2014, 2) at the maximum LWL (about 73 cm at station 1 in March 2015, and 3) before the lake dried out in July 2015. Samples from the BR and KR were collected at hydrometric stations close to the lake (marked PF and EG, respectively, in Fig. 1) five times (at the same times as SW and PW samples were collected and at two intermediate times, in February 2015 and May 2015). Shallow lake sediment samples were collected before freshwater entered the lake and at the maximum LWL.

The lake SW and PW samples were collected at three stations (marked S1, S2, and S3 in Fig. 1) along the longitudinal axis of the lake at different distances from the river inflows. Three permanent piezometers were installed at each sampling station, at 20, 50, and 100 cm depth (Fig. 3). The piezometers at each station were set 1 m apart horizontally to prevent the piezometer structures collapsing and to prevent each piezometer affecting its neighbouring device. The piezometers were installed taking care to cause minimum disturbance to the sediment and flow conditions. The lake bed is very flat and homogeneous, the shallow lake sediment being composed of thin layers (each < 3 cm thick) with different chemical and physical characteristics. The effects of small scale sediment heterogeneity on the results were eliminated using a 10 cm screen in each piezometer.

Diffusion of O_2 from the atmosphere to the PW was prevented by capping and sealing the top of each piezometer. A piezometer was pumped out several times before a PW sample was collected using a hand pump with a very low pumping rate. The potential for contaminating a PW sample with PW from different depths was minimized by placing polystyrene plates at the top and bottom of the desired sample depth (Fig. 3). However, the vertical flow rate in the lake bed sediment is very low because of its fine texture. Each river SW and PW sample was passed through a 0.45 µm cellulose acetate membrane filter, then stored in a 60 mL acid-washed polyethylene bottle and transported to the laboratory for analysis. Samples collected for As, B,

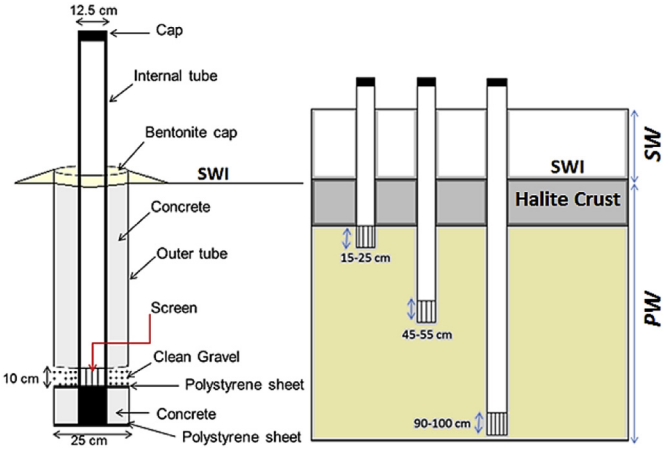

Fig. 3. Schematic of a piezometer and the pore water sampling depths (SWI: sediment–water interface, SW: surface water, PW: pore water). Each piezometer was 1 m from its nearest neighbour.

Table 1
Physicochemical parameters for the Babahaji River (BR) and Khoshk River (KR) water between November 2014 and July 2015.

Sample	Ca^{2+}	K^+	Mg^{2+}	Na^+	Cl^-	HCO_3^-	SO_4^{2-}	CB	As	B	Br	Li	EC	TDS	pH	Saturation Indices		
	mmol L^{-1}							meq L^{-1}	μg L^{-1}				mS cm^{-1}	g L^{-1}		CA	GY	HA
BR-Nov.14	3.1	0.5	3.4	6.5	3.5	12.1	2.2	0.0	1.3	325	216	25	2.4	1.5	6.9	0.2	−1.2	−6.3
BR-Feb.15	3.4	0.5	4.3	12.4	8.5	17.8	2.2	−2.4	0.7	524	485	35	3.2	2.5	7.5	1.0	−1.2	−5.7
BR-Mar.15	5.3	0.4	5.5	23.5	30.7	10.1	3.3	−1.9	1.3	555	323	28	3.6	3.0	7.3	0.5	−1.0	−4.9
BR-May.15	3.4	0.3	2.3	4.4	2.5	13.0	0.4	−0.2	1.2	568	162	16	1.4	1.2	7.3	0.7	−1.8	−6.6
BR-Jul.15	3.1	0.5	3.4	5.0	3.5	11.1	1.9	0.1	0.9	407	336	29	2.1	1.5	7.0	0.5	−1.3	−6.5
KR-Nov.14	3.3	0.4	4.1	5.4	6.2	3.9	5.3	−0.1	2.0	327	224	24	1.7	1.4	7.9	0.5	−0.9	−6.2
KR-Feb.15	5.0	0.3	4.6	11.7	12.0	7.6	5.0	1.6	0.7	535	504	38	3.0	2.3	8.0	1.3	−0.8	−5.6
KR-Mar.15	3.8	0.9	5.1	8.8	12	7.6	3.3	1.3	1.7	502	297	35	2.3	1.9	8.6	1.7	−1.1	−5.7
KR-May.15	3.5	0.3	4.4	6.8	8.3	7.8	3.3	0.2	2.5	385	270	26	2.0	1.4	7.8	1.0	−1.1	−6.0
KR-Jul.15	3.0	0.5	4.3	6.1	5.2	4.2	5.6	0.6	2.1	564	343	33	1.6	1.4	7.9	0.9	−0.9	−6.2

CB = charge balance, EC = electrical conductivity, TDS = total dissolved solids, CA = calcite, GY = gypsum, HA = halite.

Br, and Li analysis were acidified (to pH < 2) by adding ultrapure HNO_3.

Sediment samples were collected from stations S1, S2, and S3 at the maximum LWL in March 2015 and before the lake dried out in July 2015. Each surface sediment sample was collected using a clean shovel. Deep sediment samples were collected using 6 cm diameter PVC pipes in the wet season or an auger in the dry season. The cores were kept upright in a freezer while being transported from the field to the laboratory, then each core was sub-sampled by cutting it into sections. The 15–25, 45–50, and 90–100 cm sections were then placed in bags and stored for analysis. Each sediment sample was squeezed to remove excess PW, which was decanted. The sediment was then dried in air. The < 2 mm particles were isolated using a sieve and then analysed.

2.3. Measurements

The physicochemical properties (the dissolved oxygen (DO) concentration, electrical conductivity (EC), redox potential (Eh), pH, and temperature) of the water and brine samples were measured in the field using a portable HQ40d instrument (Hach, Loveland, CO, USA), and the results are shown in Tables 1, 2a, and 2b). The Eh values were corrected with respect to a hydrogen electrode.

The magnesium and calcium concentrations were measured by titrating the samples with EDTA. The sodium and potassium concentrations were determined by flame photometry (APHA, 1998). The chloride and bicarbonate concentrations were determined by titrating samples with $AgNO_3$ (the Mohr method) and HCl, respectively, and the sulphate and total dissolved iron concentrations were determined by spectrophotometry (APHA, 1998). The analyses were performed in the hydrochemical laboratory at Shiraz University. The overall quality of the ion concentrations found in a water or brine sample was checked by calculating the charge balance for the sample, and the errors for all the samples were < 5%. The As, B, Br, and Li concentrations were determined using an Agilent 7700x inductively coupled plasma mass spectrometer (Agilent Technologies, Santa Clara, CA, USA). The As, B, Br, and Li detection limits were all 1 ng L^{-1}, and the maximum dilution factor for the brine samples was 500. Several blank and standard samples were prepared and analysed to determine the accuracy of the analyses, and the results were good overall.

The sediment pH was measured using a pH meter (Pansu and Gautheyrou, 2007). Each dried sediment sample was ground and homogenized using an agate mortar and pestle to give a fine-grained homogeneous sample before the loss on ignition (LOI) and As, B, Br, and Li concentrations were determined. Each sediment sample was dried at 105 °C, then ashed at 550 °C for 2 h in a muffle furnace, and the loss on ignition was defined as the difference between the masses of the dry sample and the ashed sample (Dean, 1974). About 0.5 g of a sample was digested in 8 mL Suprapur 69% HNO_3 and 2 mL Suprapur 30% H_2O_2, and the As, B, Br, and Li concentrations in the digested sample were determined by inductively coupled plasma mass spectrometry. The quality of the As analysis was assessed by analysing the silty clay loam certified reference material CRM-SCL7003. The As concentrations (n = 2) were within ± 10% of the certified concentration.

The Fe contents of the sediment samples were determined by X-ray fluorescence analysis.

Mineral saturation indices and water densities were calculated using the PHREEQC program (Parkhurst and Appelo, 2013). The Pitzer (1987) database, which was designed for highly mineralized water and brine, was used for speciation calculations of the SW and PW samples. The results are shown in Tables 1, 2a, 2b, and 3.

3. Results and discussion

3.1. Chemical compositions and as concentrations in the inflowing river water

It was difficult to assess the water chemistry of the BR and KR because the rivers receive large but undetermined volumes of wastewater from different sources. The ECs of the BR and KR water were 1–4 mS cm^{-1} and the total dissolved solid (TDS) concentrations were 1.2–3.0 g L^{-1} (Table 1). The water in both rivers was saturated with respect to calcite and undersaturated with respect to gypsum and halite (Table 1).

Stiff diagrams (Fig. 4) indicated that the BR and KR have Mg ≈ Ca–HCO_3 and Mg ≈ Ca–SO_4 water types, respectively, at both the beginning and end of the wet season (November 2014 and July 2015, respectively). Alishvandi et al. (2011) used a hydrograph for the BR to show that the base flow contributes > 70% of the total flow of the river. The water types of the BR and KR at the beginning and end of the wet season, indicate that the BR and KR are mainly recharged by upstream carbonate aquifers (Zak and Gat, 1975), but that there are also gypsum-bearing formations (e.g., the Sachun Formation) in the KR catchment (Fig. 1). The water type of the KR changes from Ca–SO_4 upstream to Mg–SO_4 downstream because of calcite precipitation (Farjadian, 2006).

However, the TDS, Cl, and Na concentrations in the BR and KR water increased during the wet season and the water types changed to Na–Cl (Fig. 4). Industrial and municipal wastewater are almost constant sources of solutes and pollutants to the rivers, but surface runoff is seasonal and strongly affected by the climate (Vega et al., 1998). The surface runoff in the Maharlu Basin has a Na–Cl–SO_4 water type and a high TDS concentration (Bahmani, 2009; Zak and Gat, 1975), and is probably responsible for the seasonal variations in the hydrochemical water types and the TDS concentrations in the river water.

Although BR and KR receive wastewater from different sources, the Br and Li concentrations followed almost the same trend in both rivers during the study period (Fig. 5a and c). This implies that differences in the origins of the wastewater released into the rivers had little effect on

Table 2a
Dissolved major and minor element concentrations in the surface water (SW) and sediment pore water (PW) samples from station 1 (S1), station 2 (S2), and station 3 (S3) in Maharlu Lake (the locations of the sampling stations are marked on Fig. 1).

Sample Date	Depth cm	Ca^{2+}	K^{+}	Mg^{2+}	Na^{+}	Cl^{-}	HCO_3^{-}	SO_4^{2-}	CB	As	B	Br	Fe	Li	TDS
		mmol L^{-1}							eq L^{-1}	μg L^{-1}	mg L^{-1}				g L^{-1}
SW-S1															
Nov.14	5	15	8	124	4065	4050	7	102	0.19	24	5	25	2.5	0.4	251
Mar.15	38	17	16	213	5043	5500	6	89	−0.08	14	9	64	1.8	1	326
Jul.15	1	6	64	994	4718	6250	17	61	0.45	59	36	280	–	4.3	364
PW-S1															
Nov.14	20	5	50	818	5783	6500	20	333	0.62	29	30	233	6.5	3.4	419
Mar.15	20	17	17	258	4978	5550	5	99	−0.11	17	9	74	–	1.2	329
Jul.15	20	3	43	612	5553	6250	12	148	0.42	26	23	195	6.7	3	381
Nov.14	50	5	37	512	4804	5250	12	177	0.44	16	15	177	1.2	2.4	329
Mar.15	50	10	28	423	5109	5950	9	156	−0.11	24	16	137	5.4	2.1	356
Jul.15	50	3	58	880	4909	6050	18	150	0.51	44	30	240	6.8	3.7	367
Nov.14	100	6	42	699	4804	5600	3	203	0.45	17	15	199	3.4	2.7	348
Mar.15	100	8	21	288	5043	5700	5	125	−0.17	18	10	86	3.2	1.3	339
Jul.15	100	5	73	505	5506	6400	7	236	−0.04	13	12	146	2.6	1.9	392
SW-S2															
Nov.14	1	6	9	168	2196	2550	4	42	−0.04	11	6	44	2.0	0.7	150
Mar.15	33	11	19	269	5217	5900	5	104	−0.21	15	10	82	1.7	1.3	347
Jul.15	1	7	87	1206	4527	6200	15	286	0.54	66	50	392	2.1	6.5	385
PW-S2															
Nov.14	20	3	49	806	3370	4750	13	234	0.04	34	44	330	8.2	0.7	291
Mar.15	20	6	36	419	4848	5700	9	161	−0.14	122	77	649	–	1.1	342
Jul.15	20	3	92	1432	3600	5800	18	259	0.48	116	61	471	9.5	0.9	363
Nov.14	50	8	92	1436	3130	5300	22	344	0.44	52	61	472	–	0.9	333
Mar.15	50	6	107	1485	3587	5800	21	339	0.52	54	50	399	9.0	0.8	362
Jul.15	50	3	86	1232	4400	6100	20	331	0.50	73	56	452	7.7	0.8	387
Nov.14	100	5	99	1449	3050	5250	21	313	0.47	61	58	472	7.1	0.9	329
Mar.15	100	5	105	1479	3233	5500	21	339	0.44	101	61	502	–	0.9	351
Jul.15	100	3	90	1265	4213	6100	18	231	0.49	85	57	463	6.9	0.7	373
SW-S3															
Feb.15	1	27	103	233	3957	4400	3	61	0.11	11	6	77	1.2	1.2	264
Mar.15	10	16	15	269	5435	6200	3	89	−0.27	13	8	72	1.2	1.1	362
May.15	1	5	96	1373	3326	5500	19	328	0.33	60	10	130	–	1.1	341
PW-S3															
Nov.14	20	8	113	1474	2770	5100	18	365	0.36	48	66	541	35.6	8.6	323
Mar.15	20	3	114	1797	2517	5500	17	359	0.35	53	65	520	40.2	8.4	341
Jul.15	20	1	113	1856	3263	6100	21	544	0.43	67	69	560	55.3	9.4	394
Nov.14	50	4	122	1874	2252	5150	21	495	0.46	37	56	579	–	9.2	343
Mar.15	50	8	118	1838	2583	5600	16	354	0.42	56	65	555	29.8	9.3	347
Jul.15	50	4	116	1777	3788	6300	19	646	0.50	64	59	500	51.2	7.7	421
Nov.14	100	5	88	1062	4087	5750	11	297	0.25	11	28	404	17.0	6	356
Mar.15	100	3	109	1939	2748	5900	15	354	0.47	53	63	526	31.0	8.9	361
Jul.15	100	3	110	1692	3406	6300	18	603	−0.02	69	62	525	54.3	8.2	406

The sediment–water interface was classed as a depth of 0 cm, CB = charge balance, TDS = total dissolved solid concentration.

seasonal variations of the Br and Li concentrations in the water entering the Maharlu Lake from the rivers. Thus variations of the Br and Li concentrations in the rivers water could reflect the seasonal variations in surface runoff chemistry and the impact of evaporation. The EC, Br and Li concentrations and Br/Cl ratio were higher in surface runoff at the beginning of the wet season (February 2015) because residual salts on the basin surfaces (remaining from the previous period) dissolve at the beginning of the wet season, increasing the B, Br, and TDS concentrations and Br/Cl ratios in the river water more at the beginning of the wet season than later on (Fig. 5a, c, 5g, and 5h). The B, Br, and TDS concentrations and Br/Cl ratios were lower in surface runoff in the middle of the wet season than earlier in the wet season, causing the B, Br, and TDS concentrations and Br/Cl ratio to be lower in the river water in March 2015 than in February 2015 (Fig. 5a, c, 5g, and 5h). At the end of the wet season and in the dry season (May and July 2015, respectively), the B and Br concentrations, Br/Cl ratio, and EC were higher in the river water because the amount of runoff water was lower and a large proportion of the river water evaporated (Fig. 5a, c, 5g, and 5h).

The dissolved As concentrations in the river water were in the range of 0.7–2.5 μg L^{-1} (Table 1). The As concentrations were higher and more seasonally variable in the KR than in the BR (Table 1). The KR receives urban and agriculture wastewater. Only municipal wastewater drains into the KR in the dry season (Salati and Moore, 2010) and the very low flow rates of the KR in the dry season imply that negligible volumes of urban wastewater drain into the lake from this river (Fig. 2b). The BR receives mostly industrial wastewater, but the BR flow rate varies between 0 and 1 $m^3 s^{-1}$ during the dry season (May to October) (Fig. 2b).

The As concentrations in the river water varied seasonally in the opposite way to the Br and Li concentrations, the As concentrations decreased and the Br and Li concentrations increased at the beginning of the wet season because of the inflow of surface runoff in February 2015 (Fig. 5d). The input of agricultural waste water increased with the beginning of agricultural activities (January 2015) and decreased when agricultural activities ended (June 2015; Fig. 5d). Shakeri and Moore (2010) measured the As concentrations in the sediments of adjacent stretches of BR river and found higher average concentrations for As in the sediments of the stretch influenced by urban and agriculture wastewater rather than in the stretch mainly loaded with industrial effluents. The pesticide application in farmlands resulted in higher concentrations of As in the soils around the lake (Moore et al., 2009). More mass of As was transported into the Maharlu Lake by the KR (0.08 tone) than by the BR (0.05 tone) from November 2014 to July 2015,

Table 2b
Physicochemical parameters, molar ratios, and saturation indices for selected minerals in the surface water (SW) and sediment pore water (PW) samples from station 1 (S1), station 2 (S2), and station 3 (S3) in Maharlu Lake (the locations of the sampling stations are shown in Fig. 1).

Sample Date	Depth cm	pH	Eh V	T °C	DO	Na/Cl	Br/Cl	SO_4/Cl	Saturation Index						
					mg L^{-1}	Molar			CA	DO	GY	HA	GL	PO	EP
SW-S1															
Nov.14	5	7.13	0.24	17.6	0.2	1.00	7.8×10^{-5}	0.03	1.2	3.5	0.0	−0.2	−0.3	−5.6	−2.1
Mar.15	38	7.60	0.09	18.4	3.6	0.92	1.5×10^{-4}	0.02	1.5	4.6	0.4	0.5	0.9	−3.1	−1.7
Jul.15	1	7.58	0.22	30.1	2.1	0.75	5.6×10^{-4}	0.01	0.3	3.4	0.0	1.0	0.8	−1.8	−1.5
PW-S1															
Nov.14	20	6.43	−0.01	18.6	0.3	0.89	4.5×10^{-4}	0.05	0.5	4.2	0.7	1.5	3.2	2.2	−0.6
Mar.15	20	7.01	−0.08	15.3	1.8	0.90	1.7×10^{-4}	0.02	1.2	4.2	0.5	0.6	1.0	−2.6	−1.5
Jul.15	20	7.03	−0.14	31.9	0.9	0.89	3.9×10^{-4}	0.02	0.4	3.9	−0.1	2.6	1.4	−1.6	−1.3
Nov.14	50	6.14	−0.03	19.4	0.5	0.92	4.2×10^{-4}	0.03	0.4	3.4	0.1	0.5	0.8	−2.0	−1.1
Mar.15	50	7.01	−0.12	14.4	1. 7	0.86	2.9×10^{-4}	0.03	1.0	4.3	0.6	0.8	1.6	−0.8	−1.0
Jul.15	50	6.88	−0.16	31.8	0.4	0.81	5.0×10^{-4}	0.02	0.5	4.3	−0.1	0.9	1.2	−1.4	−1.2
Nov.14	100	6.6	−0.02	19.6	0.8	0.86	4.4×10^{-4}	0.04	0.1	2.5	0.3	0.8	1.4	−0.7	−0.9
Mar.15	100	7.06	−0.08	16.6	2.1	0.88	1.9×10^{-4}	0.02	0.9	3.9	0.3	0.6	1.0	−2.4	−1.4
Jul.15	100	6.77	−0.15	30.6	0.4	0.86	2.9×10^{-4}	0.04	0.4	3.7	0.4	1.1	2.1	0.4	−1.1
SW-S2															
Nov.14	1	7.51	−0.06	15.4	0.8	0.86	2.2×10^{-4}	0.02	0.3	2.3	−1.0	−1.0	−2.6	−8.7	−2.3
Mar.15	33	7.69	0.12	16	5.7	0.88	1.7×10^{-4}	0.02	1.1	4.2	0.4	0.7	1.2	−2.2	−1.4
Jul.15	1	7.08	−0.03	42	1.0	0.73	7.9×10^{-4}	0.05	−0.0	3.2	0.4	1.1	2.1	0.9	−0.8
PW-S2															
Nov.14	20	7.43	−0.20	17.2	0.5	0.71	8.7×10^{-4}	0.05	0.5	4.0	−0.2	0.2	0.1	−2.3	−0.7
Mar.15	20	7.48	−0.09	16.2	2.6	0.85	1.4×10^{-3}	0.03	0.9	4.2	0.3	0.7	1.1	−1.5	−1.1
Jul.15	20	7.11	−0.19	34.9	0.4	0.62	1.0×10^{-3}	0.04	0.1	3.7	0.0	0.9	1.4	−0.2	−0.9
Nov.14	50	6.91	−0.18	15.2	0.3	0.59	1.1×10^{-3}	0.06	0.7	4.4	0.6	0.6	1.5	1.2	−0.2
Mar.15	50	6.99	−0.10	16.4	2.0	0.62	8.6×10^{-4}	0.06	0.5	4.2	0.7	0.9	2.1	2.1	−0.2
Jul.15	50	6.69	−0.15	33.2	0.4	0.72	9.3×10^{-4}	0.05	0.2	4.0	0.2	1.1	1.9	0.6	−0.7
Nov.14	100	6.93	−0.15	17.2	0.2	0.58	1.1×10^{-3}	0.06	0.5	4.2	0.3	0.6	1.2	0.5	−0.4
Mar.15	100	7.01	−0.10	16.5	2.5	0.59	1.1×10^{-3}	0.06	0.4	4.1	0.5	0.8	1.7	1.3	−0.3
Jul.15	100	7.06	−0.14	33.6	0.4	0.69	9.5×10^{-4}	0.04	0.1	3.7	0.0	1.0	1.5	−0.1	−0.9
SW-S3															
Feb.15	1	7.77	0.16	12.4	6.9	0.90	2.2×10^{-4}	0.01	1.3	3.9	0.1	0.0	−0.4	−3.2	−1.9
Mar.15	10.4	7.57	0.17	16.8	7.0	0.88	1.5×10^{-4}	0.01	1.0	3.8	0.7	0.9	1.6	−1.8	−1.5
May.15	1	7.17	0.12	31.3	2.5	0.60	3.0×10^{-4}	0.06	0.5	4.2	0.3	0.6	1.3	0.3	−0.6
PW-S3															
Nov.14	20	7.09	−0.20	18.2	0.9	0.54	1.3×10^{-3}	0.07	0.6	4.3	0.5	0.5	1.3	1.1	−0.3
Mar.15	20	7.25	−0.09	13.7	1.5	0.46	1.2×10^{-3}	0.07	0.0	3.7	0.4	0.7	1.4	1.5	−0.1
Jul.15	20	6.72	−0.24	33.5	0.4	0.53	1.1×10^{-3}	0.09	−0.8	2.8	−0.1	1.1	1.8	1.1	−0.3
Nov.14	50	6.63	−0.13	15.3	0.9	0.44	1.4×10^{-3}	0.10	0.2	3.9	0.5	0.7	1.6	1.9	0.0
Mar.15	50	7.09	−0.07	14.2	2.1	0.46	1.2×10^{-3}	0.06	0.4	4.0	0.8	0.8	2.0	2.5	−0.1
Jul.15	50	6.75	−0.15	35.1	0.5	0.60	9.9×10^{-4}	0.10	0.4	4.2	0.9	1.0	2.3	3.0	
Nov.14	100	6.4	−0.18	18	1.0	0.71	8.8×10^{-4}	0.05	0.3	3.6	0.5	0.8	1.7	0.9	−0.5
Mar.15	100	7.00	−0.05	14.7	2.2	0.47	1.1×10^{-3}	0.06	−0.3	3.2	0.5	1.0	1.9	2.1	−0.1
Jul.15	100	6.66	−0.20	33.7	0. 8	0.54	1.0×10^{-3}	0.10	−0. 7	2.7	0.4	1.1	2.4	2.3	−0.3

The sediment–water interface was classed as a depth of 0 cm, T = temperature, TDS = total dissolved solid concentration, CA = calcite, DO = dolomite, GY = gypsum, HA = halite, GL = glauberite, PO = polyhalite, EP = epsomite.

(Khosravi, 2018). We conclude that the release of agricultural wastewater into the rivers (predominantly from the KR) is the most important anthropogenic source of As for Maharlu Lake.

Najmodini (2011) found dissolved As concentrations of 4–5 and 2–3 μg L^{-1} in the rivers flowing into the Maharlu Lake and three springs in the Maharlu Basin, respectively. The As concentrations were 1.5–2 times higher in the river water than in groundwater in the basin. It can be probably due to wastewater loadings to rivers and evaporation. However, generally the As concentrations in the river water varied markedly from year-to-year in response to annual changes in temperature and precipitation.

3.2. Chemical compositions of the Maharlu Lake SW and PW

The Maharlu Lake SW and PW were neutral (pH 6–8) and Na–Mg–Cl–SO_4 brines with TDS of 150–420 g L^{-1} (Tables 2a and 2b). The SW and PW were depleted in HCO_3 and Ca and the Eh values varied between anoxic and suboxic (Tables 2a and 2b). The data indicated that the SW and PW were in the halite precipitation stage at most places throughout most of the sampling period (Khosravi et al., 2018). In this evaporative evolution stage for a Na–Cl brine, Mg and Br behave as conservative species, i.e., they do not participate in the precipitation of minerals (Eugster and Jones, 1979; McCaffrey et al., 1987) and their concentrations increase as water continues to evaporate from the brine. However, the Na concentration decreases as more evaporation occurs because Na precipitates in halite and as Na sulphates such as glauberite.

The TDS values was strongly positively correlated with the Cl concentration (Fig. 6a) and increased slightly with the Mg concentration (Fig. 6d). The Na concentration was not correlated with the Cl concentration, and most of the SW and PW samples had Na/Cl molar ratios < 1 (Fig. 6b). This is consistent with the positive saturation indices found for glauberite ($Na_2Ca(SO_4)_2$), as shown in Table 2b, suggesting that glauberite would have precipitated. Glauberite does not contain Cl, which remains in the brine as a conservative species. The Na concentration was significantly negatively correlated with the Mg concentration (Fig. 6e). The Br/Cl molar ratio did not correlate with the Cl concentration but was strongly positively correlated with the Mg concentration (Fig. 6c and f). In general, the Mg concentrations and Br/Cl molar ratios were lower in the lake SW than in the PW because the SW was less affected than the PW by evaporation (Fig. 6). Interactions between the SW and PW decrease the effective degree of evaporation of the PW and also decrease the Mg concentration and the Br/Cl molar

Table 3
As, B, Br, Fe, and Li contents, losses on ignition (LOIs; %), and pH values of the solid phases of the surface and shallow sediment samples from station 1 (S1), station 2 (S2), and station 3 (S3) in Maharlu Lake (the locations of the sampling stations are shown in Fig. 1).

Sample Date Depth (cm)	Fe% wt	Li	B	Br	As	LOI%	pH	General texture of sediment samples
		μg/g						
S1-Mar.15								
0–5	–	0.0	< 3.9	8.3	< 0.025	0.4	8.19	Pure Crystalline Halite
20	–	1.0	94.5	35.9	6.1	3.3	9.04	Silt–Clay
50	–	2.5	105.1	54.3	5.1	9.7	8.59	Silt–Clay
100	–	3.8	81.2	31.1	5.1	12.6	8.75	Silt–Clay
S1-Jul.15								
0–5	0.0	0.1	< 3.9	5.3	< 0.025	1.1	8.53	Pure Crystalline Halite
20	1.4	1.1	73.0	31.5	3.9	8.9	9.13	Silt–Clay
50	1.8	1.7	110.0	47.1	6.3	11.3	9.10	Silt–Clay
100	6.1	1.7	45.2	21.8	3.0	13.3	8.81	Silt–Clay
S2-Mar.15								
0–5	–	0.1	< 3.9	2.7	< 0.025	9.5	8.30	Pure Crystalline Halite
20	–	1.4	125.9	36.2	0.9	8.7	9.00	Crystalline Evaporites
50	–	1.4	114.7	32.2	0.9	12.4	8.74	Crystalline Evaporites
100	–	1.2	110.4	28.2	0.7	16.0	8.60	Crystalline Evaporites
S2-Jul.15								
0–5	0.0	0.2	7.5	5.1	0.0	1.1	8.46	Pure Crystalline Halite
20	0.0	0.1	< 3.9	4.1	< 0.025	2.3	8.58	Crystalline Evaporites
50	0.3	0.8	52.8	15.7	0.5	3.5	8.83	Crystalline Evaporites
100	0.4	0.8	70.1	14.6	0.5	4.6	8.57	Crystalline Evaporites
S3-Mar.15								
0–5	–	0.0	< 3.9	3.7	< 0.025	1.2	8.59	Pure Crystalline Halite
20	–	4.1	310.2	58.5	6.4	4.0	8.39	Silt–Clay
50	–	3.7	255.1	49.8	4.6	11.0	8.24	Silt–Clay
100	–	3.9	213.5	41.9	5.7	15.0	7.86	Silt–Clay
S3-Jul.15								
0–5	0.0	0.1	< 3.9	4.1	< 0.025	1.5	8.33	Pure Crystalline Halite
20	0.3	0.5	31.4	13.3	0.5	2.8	8.32	Silt–Clay
50	1.6	2.1	142.5	30.8	3.5	10.0	8.23	Silt–Clay
100	2.3	3.4	214.5	43.7	4.7	13.3	8.11	Silt–Clay

ratio (Khosravi et al., 2018).

The Br/Cl ratios, Mg concentrations, and TDS values in the PW samples increased but the Na concentrations decreased as distance from the river inflow points increased (Fig. 6). This implies that the degree to which evaporation had affected the PW increased as the distance from river inflow areas increased (Khosravi et al., 2018). The DO

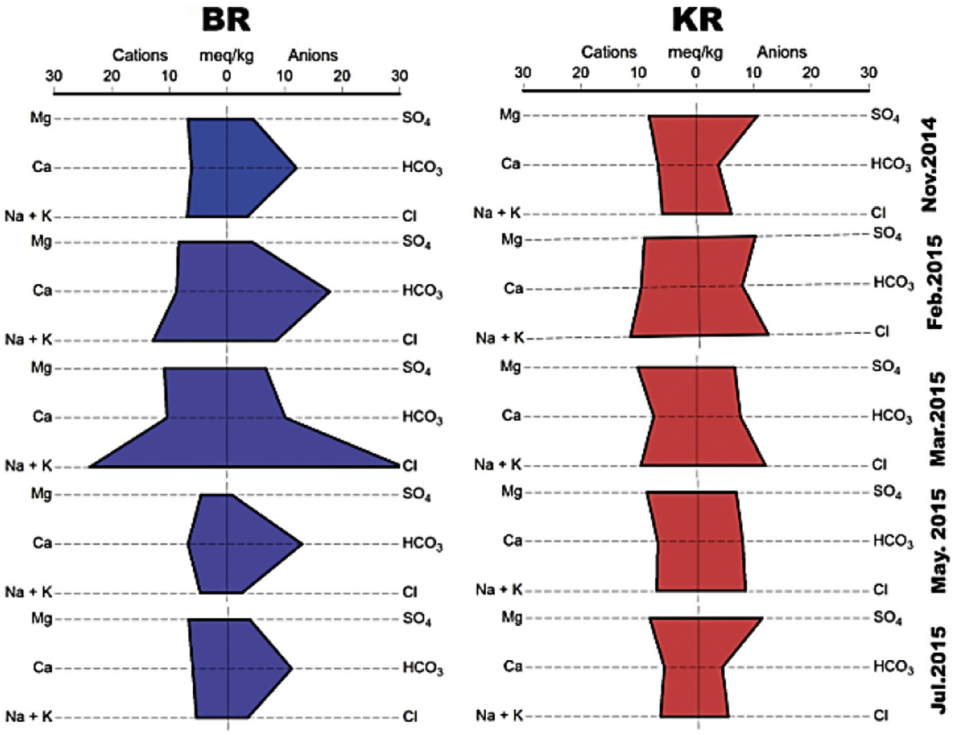

Fig. 4. Stiff diagrams for Babahaji River (BR) and Khoshk River (KR) and variations of the water types of the rivers during the study period (November 2014 to July 2015).

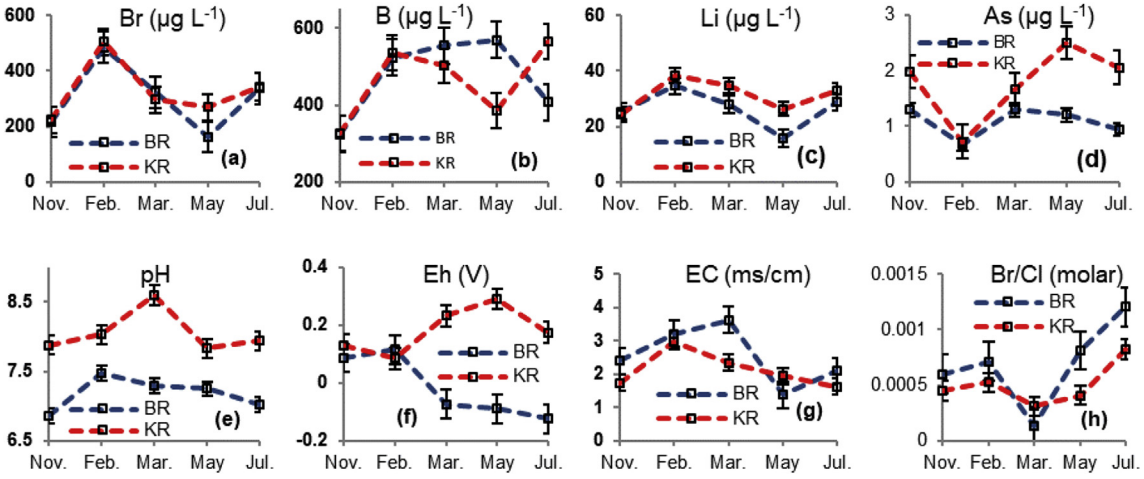

Fig. 5. a) Br concentrations, b) B concentrations, c) Li concentrations, d) As concentrations, e) pH, f) redox potentials (Eh), g) electrical conductivities (EC), and h) Br/Cl molar ratios in the Khoshk River (KR; red dashed lines) and Babahaji River (BR; blue dashed lines) during the study period (November 2014 to July 2015). (For interpretation of the references to colour in this figure legend, the reader is referred to the Web version of this article.)

concentration in the PW increased, changing the redox conditions, as the LWL increased (Fig. 7). Increasing the DO concentration caused the Eh value for the PW at station 3 to increase (Fig. 7).

In general, the Eh and DO concentration in the PW decreased as the depth increased (Fig. 7). The Eh and DO concentration were much higher in the SW than in the PW (Fig. 7), but they decreased as the amount of evaporation increased because O_2 becomes less soluble as the temperature increases. Even when the lake SW completely evaporates in the dry season the crystalline halite crust prevents contact between the sediment and O_2 in the atmosphere. The DO concentrations in the lake SW and PW increased during the wet season (Fig. 7).

3.3. As distribution across the SWI

The shallow sediment at the centre of Maharlu Lake is composed of crystalline evaporites (halite and sulphates such as gypsum and glauberite), and the sediment near the shore is composed of carbonates, aluminosilicates, and evaporites (Table 4 Khosravi (2018)). A strong correlation was found between the As and Fe contents of the solid phases of the sediment samples (Fig. 8a), suggesting that As was incorporated into iron sulphide phases such as mackinawite ($Fe_{0.75}Ni_{0.25}S_{0.9}$) and pyrite ($FeS_2$) or into iron oxy-hydroxides. However, iron (hydr)oxides are not stable at the Eh values found, ~ −200 mV (Appelo and Postma, 2005; Sracek et al., 2018). The low Eh values of the sediment samples (Fig. 7) and the availability of sulphate indicate that iron sulphides are more likely than iron (hydr) oxides to be present in the Maharlu Lake sediment. This view was supported by the strong sulphide smell of the sediment and water samples and black sediment coatings that disappeared on contact with the atmosphere. The As–Fe–S phase is dominant in the Maharlu Lake sediments across the SWI (Khosravi, 2018). This agrees with the results of other geochemical studies that have shown that the incorporation of As into iron sulphides is an important mechanism through which As is sequestered in anoxic environments, in which Fe(III) oxides are

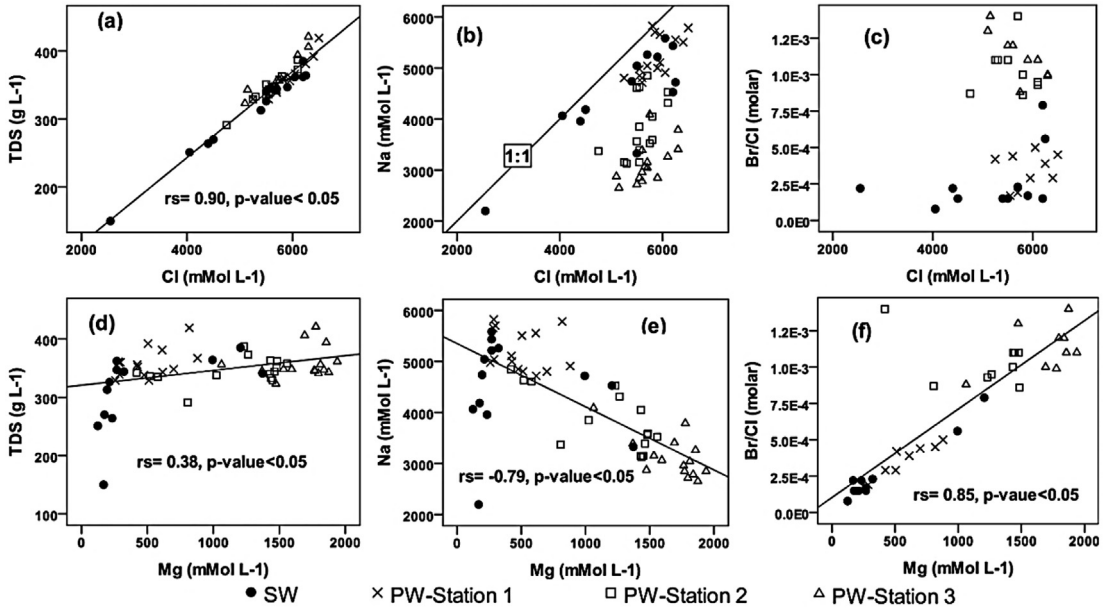

Fig. 6. Correlations between the (a) total dissolved solid (TDS) and Cl concentrations, (b) Na and Cl concentrations, (c) Br/Cl ratios and Cl concentrations, (d) TDS and Mg concentration, (e) Na and Mg concentrations, and (f) Br/Cl ratios and Mg concentrations in the surface water (SW) and sediment pore water (PW) samples from Maharlu Lake (rs is the Spearman correlation coefficient, p-values < 0.05 were considered to indicate significant correlations; the lines are fitted to all the points).

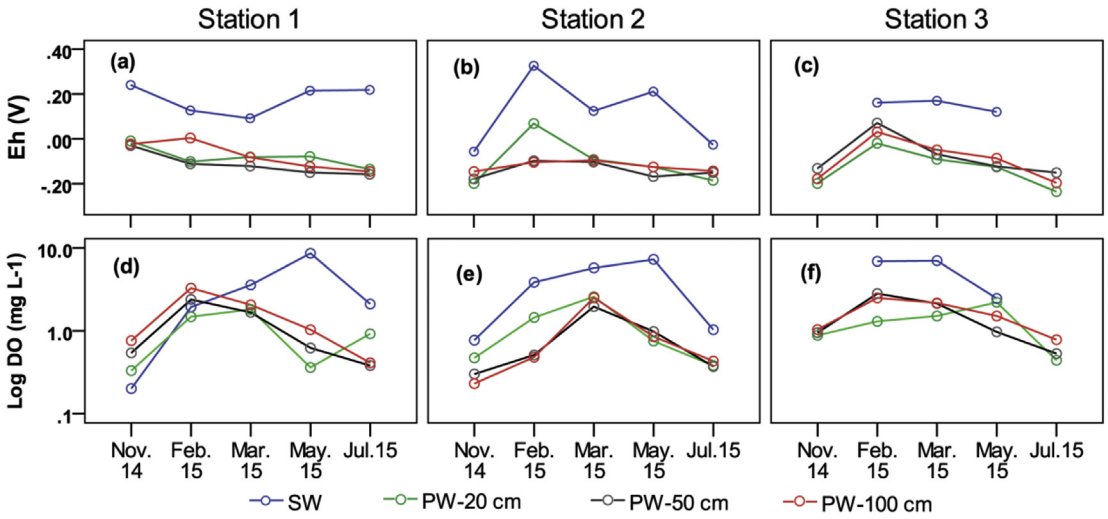

Fig. 7. Redox potentials (Eh) and log (dissolved oxygen concentrations) (log DO) of the sediment pore water (PW) samples from (a) and (d) station 1, (b) and (e) station 2, and (c) and (f) station 3 at different depths plotted against time during the study period.

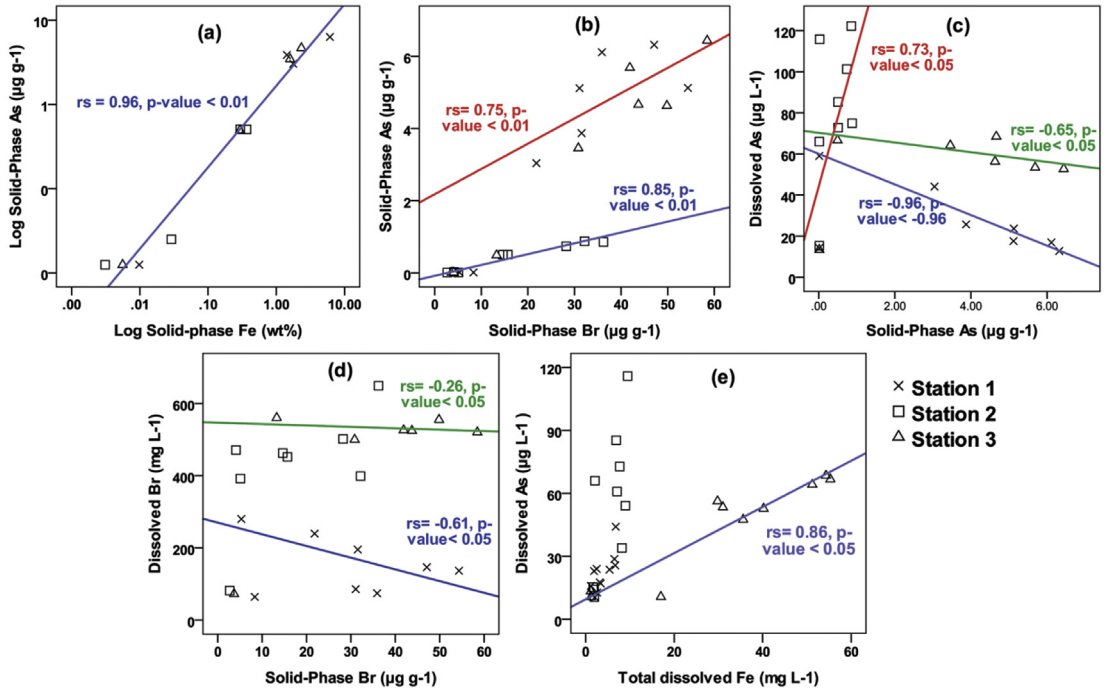

Fig. 8. (a) Solid-phase As contents plotted against the solid-phase Fe contents, (b) solid-phase As contents plotted against the solid-phase Br contents, (c) dissolved-phase As concentrations plotted against the solid-phase As contents, (d) dissolved-phase As concentrations plotted against the solid-phase Br contents, and (e) dissolved-phase As concentrations plotted against the total dissolved Fe concentrations for the samples from stations 1, 2, and 3 (rs is the Spearman correlation coefficient, and p-values < 0.05 were considered to indicate significant correlations; the lines were fitted to all points using SPSS software).

unstable (Couture et al., 2010; Wilkin and Ford, 2006). The black organic-rich zone in marine sediment is an anoxic non-pyritic mono-sulfide environment, and the green or gray zone is a pyrite environment (Berner, 1970). Similar sequences have been found in SWIs in other salt lakes (Lyons and Lebo, 1996).

Comparing the dissolved and solid-phase As distributions with the distributions of a typical conservative element such as Br could help to assess the roles of different processes in the behavior of As. Variations in the dissolved Br concentration in a saline system reflect the effects of hydrological processes such as evaporation, dilution, and mixing, but also its input from degradation of organic matter (OM, McArthur et al., 2012). The incorporation of Br into the halite structure may affect the Br concentration (McCaffrey et al., 1987), but the process is limited and halite precipitation increases the Br/Cl ratio (Davis et al., 1998; Cartwright et al., 2006).

The As and Br contents of the solid phases of the sediment samples were strongly positively correlated (Fig. 8b). The SWI sediment could be divided into two groups given the relationships between the As and Br contents of the solid phases of the sediment samples. Group 1 included pure halite surface crust and crystalline evaporites at station 2. This group had relatively low As and Br contents in the solid phase, and the As concentration increased with Br content. Group 2 included non-evaporitic sediment (e.g., aluminosilicates) and poorly soluble evaporites (e.g., carbonates). This group had relatively high As and Br contents, and the As content increased at a higher rate than the As content for group 1 as the Br content increased.

Pure evaporites sorb very limited amounts of As, and negligible amounts of As are incorporated into most evaporite minerals (Welch and Lico, 1998). This explains why the lowest As contents of the solid phase sediment, but the highest dissolved As concentrations in sediment PW, were found at station 2 (Fig. 8c).

These observations are supported by the results of Ong et al. (1997), who found that As, B, Mo, and Se were largely excluded from evaporite minerals and accumulated in highly evapo-concentrated water in agricultural wastewater evaporation ponds in the San Joaquin Valley, California. This resulted in trace element concentrations being relatively low in evaporites and relatively high in brine.

The As and Br contents of the solid phase sediment from stations 1 and 3 were within similar ranges, but the dissolved As and Br concentrations were higher in pore water from station 3 than in pore water from station 1 because the pore water at station 2 and especially at station 3 had been more affected by evaporation than the brine from station 1 (Fig. 8c and d). This is also indicated by increasing Br/Cl ratios from PW1 to PW3 (Fig. 6c). The dissolved As and Br concentrations in sediment from station 1 decreased as the As and Br contents of the solid phase increased. However, the dissolved As concentration in sediment from station 3 decreased slightly as the As content of the solid phase increased, and the dissolved Br concentration remained constant as the Br content of the solid phase increased (Fig. 8c and d). The dissolved As and total dissolved Fe concentrations were poorly correlated in sediment from stations 1 and 2, but significantly positively correlated in pore water from station 3 (Fig. 8e).

The dissolved As and Br concentrations and the As and Br contents of the solid phase for sediment from station 1 indicated that the As behaved in a similar way to typical conservative solutes such as Br. The mobility of dissolved As in the environment is largely controlled by redox conditions, which govern the As oxidation state and the thermodynamic stability of As in the solid phase (Baviskar et al., 2015). The general distributions of dissolved As concentrations in the SW and PW in Maharlu Lake were not clearly related to the Br/Cl ratio, Eh, Na/Cl ratio, pH, SO_4 concentration, or TDS (Fig. 9). However, trends were found in the relationships between the As concentration and some parameters at each station (indicated with arrows in Fig. 9).

The evaporative evolution of brine, the dissolution and precipitation of very soluble evaporites, and the diagenetic evolution of carbonates are the main processes controlling the SW and PW chemistry in Maharlu Lake (Khosravi et al., 2018).

In most SW and PW samples from station 1 the As concentration increased as the Br/Cl ratio, Mg concentration, halite saturation index, polyhalite saturation index, and TDS increased, but decreased as the Na/Cl ratio decreased (Fig. 9). At station 2, the As concentration in the PW increased as the Br/Cl ratio and Mg concentration increased, decreased as the Na/Cl ratio decreased, and slightly decreased as the halite saturation index, polyhalite saturation index, and TDS decreased (Fig. 9). The interpretation of Br/Cl ratio is a useful indicator of redox processes. When evaporation occurs, its value remains constant. In contrast, its increasing value might indicate degradation of organic matter in redox processes (Davies at al., 1998,; Cartwright et al., 2006; McArthur et al., 2012; Jia et al., 2017). The Br/Cl ratios in SW and PW1 remained almost constant in parallel with increasing Cl^- concentrations, but increased sharply at PW2 and especially at PW3 (Fig. 6c). This is consistent with As concentrations which are lower in SW and PW1 where Br/Cl ratios are also low, but both values increase at PW2 and at PW3 (Fig. 8e), indication a dominant role of evaporation in SW and PW1 and redox processes operating in parallel with evaporation at PW2 and PW3.

The As concentration in an aquatic system can increase because of evaporation. This can, for example, affect shallow aquifers in semiarid regions (Welch and Lico, 1998; Zabala et al., 2016), evaporation basins (Gao et al., 2007; Ryu et al., 2010), and SW and shallow groundwater in dry salt lakes (Hacini and Oelkers, 2011; Ryu et al., 2002). The dissolved As concentration in such a system is positively correlated with the concentrations of conservative solutes such as Cl, Br, and Li or with the EC of the water. The dissolved As concentrations and TDS in most of the SW and PW samples from station 1 increased as the effect of evaporation increased. For the PW from station 2, the increasing effect of evaporation caused the As concentration to increase, but the TDS to decrease because of the precipitation of halite and other minerals such as polyhalite.

The results indicate that evaporative evolution is an important mechanism controlling dissolved As concentrations in SW and PW at stations 1 and 2.

Dissolved As behaved differently at station 3, decreasing as the pH, Eh, Br/Cl ratio, Mg concentration, calcite saturation index, and dolomite saturation index increased and increasing as the Na/Cl ratio and total dissolved Fe and SO_4 concentrations increased (Figs. 8e and 9). The dissolved Br concentration at station 3 remained constant as the Br content of the solid phase changed, implying that the brine at this station is at equilibrium with solid phase evaporites and that hydrological processes have limited effects (Fig. 8d). The dissolved As concentration decreased slightly as the As content of the solid phase increased and increased as the total dissolved Fe concentration increased (Fig. 8c, d, and 8e), indicating that the dissolved As concentration at station 3 is controlled mostly by solid phase reactions like precipitation of secondary sulphides incorporating As.

Mixing of PW with SW reduces the degree evaporation of the brine, the Br/Cl ratio, and the Mg concentration, but increases the Na/Cl ratio. However, limited SW–PW mixing occurs at station 3. The natural evaporites may be very porous, and reactions with interstitial brine may therefore be important in the early stages of diagenesis (McCaffrey et al., 1987). Reactions between brine and gypsum (or anhydrite) during the evaporation of seawater can cause glauberite ($Na_2Ca(SO_4)_2$) and polyhalite ($K_2MgCa_2(SO_4)_4.2H_20$) to form (Eugster, 1980). The formation of these secondary sulphates, particularly polyhalite, can strongly affect the subsequent evolution of the evaporating brine (McCaffrey et al., 1987). Polyhalitization of previously deposited gypsum occurs through the reaction shown in eq. (1) (Hardie, 1984).

$$2CaSO_4.2H_2O_{(s)} + 2K^+(aq) + Mg^{2+}{}_{(aq)} + 2SO_4{}^{2-}{}_{(aq)} \rightarrow 2CaSO_4.MgSO_4.2KSO_{4(s)} + 2H_2O_{(l)} \quad (1)$$

The increasing SO_4 concentration and Na/Cl ratio but decreasing Mg concentration and Br/Cl ratio, as the dissolved As concentration in the PW increased, appeared to be caused by reactions between the brine and precipitated evaporites such as gypsum, causing new secondary sulphates to precipitate, and it appears that very limited SW infiltration occurs at station 3. These reactions decreased the dissolved As concentration in PW at station 3. The calcite and dolomite saturation indices in the PW at station 3 increased because the Ca concentration increased as a consequence of dissolving gypsum. This process inversely affected (i.e., decreased) the dissolved As concentration.

Under strongly reducing conditions, sulphate is reduced and As can be incorporated into several sulphide minerals (Appelo and Postma, 2005; Sracek et al., 2004). The positive correlation between the As and SO_4 concentrations may have been caused by evaporation (causing the concentrations of both solutes to increase) but also by sulphate reduction, causing As to become associated with secondary sulphides (both solutes being scavenged simultaneously into the solid phase) (Sracek et al., 2018). Relatively low arsenic concentrations at PW1 and low and almost constant SO_4/Cl ratio suggest there is no sulphate reduction (Fig. 10a). At PW2 constant SO_4/Cl ratio suggests both evaporation and sulphate reduction operate in parallel. At PW3 slightly increasing SO_4/Cl ratio in parallel with increasing arsenic concentration suggests that evaporation with halite precipitation are more important than sulphate reduction. In the SO_4 vs. SO_4/Cl plot (Fig. 10b) there is a steady increasing trend from SW through PW1, PW2 towards PW3, indicating that evaporation and precipitation of halite are more important than sulphate reduction. However, sulphate reduction does occur as

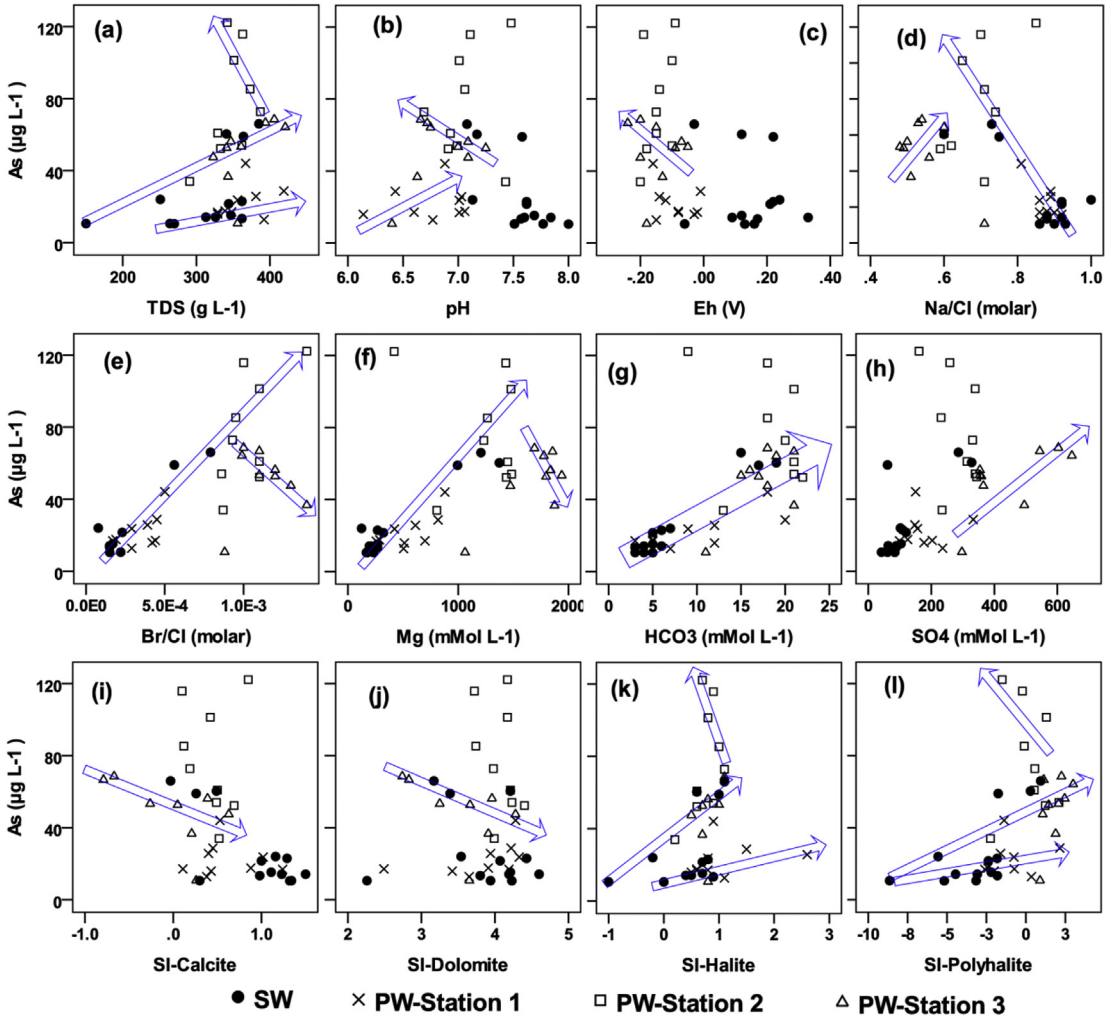

Fig. 9. Relationships between the dissolved As concentrations and the (a) total dissolved solid (TDS) concentrations, (b) pH values, (c) redox potentials (Eh), (d) Na/Cl ratios, (e) Br/Cl ratios, (f) Mg concentrations, (g) HCO_3 concentrations, (h) SO_4 concentrations, (i) calcite saturation indices (SI-Calcite), (j) dolomite saturation indices (SI-Dolomite), (k) halite saturation indices (SI-Halite), and (l) polyhalite saturation indices (SI-Polyhalite) for the surface water (SW) and sediment pore water (PW) samples from Maharlu Lake. The arrows illustrate possible trends.

indicated by the high reduced sulfur content in sediments. In salt lakes, evapo-concentration increases the sulphate concentration faster than it is decreased through sulphate reduction (Ryu et al., 2002). Sulphate reduction decreases the dissolved sulphate concentration in a system and increases the dissolved sulphide concentration, an important process regulating redox conditions in sediment PW in dry salt lakes such as Owens Dry Lake (Ryu et al., 2002). In some cases, sulphate-reducing bacteria can reductively dissolve As-rich ferric oxyhydroxides (Fan et al., 2018). However, Oren (1999) indicated low-energy-yielding anaerobic processes such as sulphate reduction are not important in salt-saturated ecosystems. The theory proposed by Oren (1999) was supported by research performed by Kulp et al. (2006) at the hypersaline Searles Lake, USA.

The increasing dissolved As concentration as the Eh and pH decreased implies that the behavior of As at station 3 was caused by the dissolution of iron oxy-hydroxides. Abiotic reductive dissolution of iron

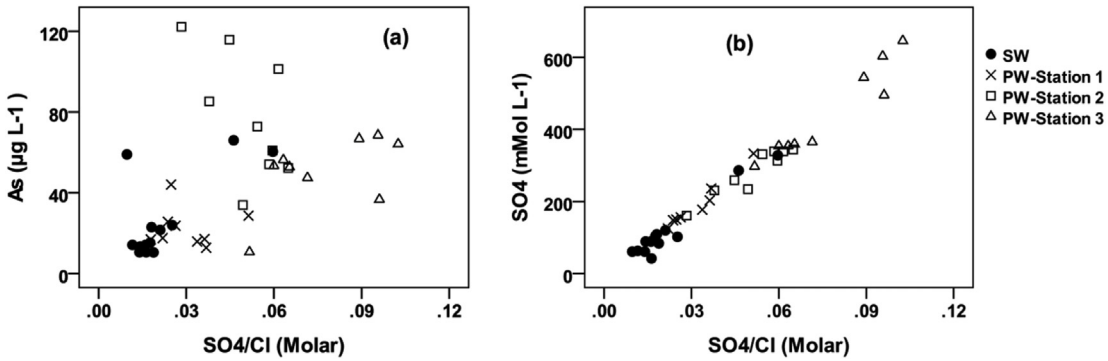

Fig. 10. Relationships between a) dissolved As and SO_4/Cl ratio and b) SO_4 and SO_4/Cl ratio.

oxy-hydroxides cause Fe and As to be mobilized and released into aquatic systems. This mechanism has been shown to be the most likely to cause high As concentrations in aquifers in West Bengal and Bangladesh (Bose and Sharma, 2002; von Brömssen et al., 2007). It seems that the changes in dissolved As concentration at station 1 and 2 are not controlled by redox and solid-phase processes such as adsorption and coprecipitation and that these processes have negligible effects on the dissolved As concentration. However, they play important roles at station 3 far from the river inflows into the lake.

3.4. Seasonal variations in as concentrations across the SWI

The high surface-to-volume ratios of temporary salt lakes make such lakes sensitive to seasonal and short-term environmental changes (Garcia and Niell, 1993). Variations in the hydrological budgets of salt lakes also cause marked inter-annual changes (Hammer, 1986). Conservative As behavior despite the presence of Fe-rich particles and the predominance of hydrodynamic over geochemical constraints on seasonal fluctuations in As concentrations in the SW column of a subtropical reservoir were described by Brandenberger et al. (2004). Hydrodynamic changes such as LWL fluctuations may also affect As concentrations.

Br is a good tracer of hydrological events such as evaporation and dilution in Maharlu Lake (Khosravi et al., 2018). Variability in the Br profile during the LWL fluctuation period decreased as distance from the inflow points increased (i.e., from station 1 to station 3). This indicates that the effects of hydrological processes decrease as the distance from inflow points increases. At station 1, near to the rivers, rapid downward infiltration of SW into shallow PW occurs during the wet season when the LWL increases. In contrast, at station 3, far from the rivers inflow, very limited interactions between SW and PW occur (unpublished data).

Significant differences were found between the Eh values for the SW and PW, and the PW Eh values were in the anoxic range (Fig. 11j–11l). The Eh decreased during the study period (November 2014 to July 2015) at station 1 (Fig. 11j), but the Eh values at stations 2 and 3 increased as the LWL increased from November 2014 to March 2015 and decreased as the LWL decreased again from March 2015 to July 2015 (Fig. 9k–l). Variations of vertical profile in the Br, As, and SO_4 concentrations in the SW and PW as the LWL fluctuated (Fig. 11a and c, 11d–11f, and 11g–11i, respectively) were not similar to variations in Eh.

Variations in the dissolved As concentration depth profiles as the LWL fluctuated were different at the different stations (Fig. 11d and f). At station 1, the dissolved As concentration did not change over time or with depth between November 2014 and March 2015. The As concentration decreased with depth in a similar way to the Br concentration in July 2015. The SO_4 concentration profiles varied in similar ways to the Br profiles in November 2014 and March 2015 but followed the opposite trend with depth in July 2015. The precipitation of sulphates caused by increased evaporation of the brine occurred in July 2015, decreasing the SO_4 concentration. This implies that the dissolved SO_4 concentration across the SWI is mostly controlled by the degree to which evaporation has affected the brine and by SW–PW mixing.

At station 2, the As and Br concentration depth profiles were similar at different times. The dissolved SO_4 concentration depth profile was similar to the As and Br concentration profiles in November 2014 and March 2015 but followed the opposite trend in July 2015 (Fig. 11g and i). The As behavior is conservative, like the Br behavior, at station 2 because no adsorption or co-precipitation of As occurs, given that the SWI layer at station 2 is composed of evaporites.

At station 3, the Br concentration profile did not change over time but the As concentration in the total water column increased over the study period (Fig. 11d and f). The Br concentration profiles indicate that the degree to which evaporation affected the PW decreased as the depth increased (Fig. 11a and c). The As and SO_4 concentrations increased in July 2015.

Variations in the As, Br, and SO_4 concentration and Eh profiles as the LWL fluctuated were assessed, and some relationships were found between the dissolved As concentrations and the other parameters. However, variations in the Eh did not consistently affect the dissolved As concentration.

The mean As concentration in the lake SW in July 2015 was about 62 $\mu g\,L^{-1}$, and the mean As concentration in the lake SW in May 2010 was about 187 $\mu g\,L^{-1}$ (Najmodini, 2011). These measurements were both made shortly before the lake became completely dry. The difference between the concentrations in 2010 and 2015 implies that the dissolved As concentration in the Maharlu Lake SW varies considerably year-to-year. Precipitation and evaporation in the basin were 249 and 2353 mm, respectively, in 2015, and 107 and 2443 mm, respectively, in 2010. We conclude that inter-annual variations in the As concentration in the lake SW are caused by different degrees of evaporation and dilution because annual precipitation in the Maharlu Basin is rather variable.

4. Conclusions

The results indicate that changes in surface runoff and agricultural wastewater inputs change the hydrochemical water type and TDS concentration in Maharlu Lake. The As concentration in the inflowing river water decreased as the contribution of surface runoff to the total river flow increased. The As concentration increased when agricultural activities in the basin started and decreased when they ended. The As concentrations were higher in the KR than in the BR because the KR receives mostly urban and agricultural wastewater whereas the BR receives mostly industrial wastewater.

The SWI at station 2 is composed of crystalline evaporites, so the dissolved As concentration was higher at station 2 than at the other stations but the As content of the sediment solid phase at station 2 was low.

Evaporation affects station 3 more than station 1, resulting in the dissolved As and Br concentrations being higher at station 3 than at station 1, although the concentrations were in similar ranges at both stations. The dissolved As concentration at station 1was constant as the As content of the solid phase increased, implying that the dissolved As concentration at this station is not controlled by solid-phase processes such as adsorption and coprecipitation. In contrast, the dissolved As concentration at station 3 decreased slightly as the As content of the solid phase increased, suggesting that the dissolved As concentration at this station is controlled mostly by solid-phase reactions. The strong correlation between the As and Fe contents of the sediment solid phase confirmed that As is incorporated into iron sulphides such as mackinawite and pyrite.

The dissolved As concentrations in SW and PW at station 1 are mostly controlled by hydrological processes such as evaporation and SW–PW mixing as suggested by Br/Cl ratio vs. Cl^- plot. However, the dissolved As concentration in PW at station 2 and especially station 3 is partly controlled by reactions between residual brine and sulphate minerals such as gypsum, producing secondary Na-, K-, and Mg-bearing sulphate minerals. Furthermore, redox reactions such as sulphate reduction in reaction with organic matter in sediments, as suggested by the increasing Br/Cl ratio, increased the Fe, S and As concentrations in the sediments and causes a sequestration of dissolved As into secondary sulfides.

In conclusion, the As distribution across the SWI in the hypersaline Na–Cl Maharlu Lake is controlled mostly by hydrological processes such as evaporation and interactions between SW and PW at stations close to freshwater (river) inflow areas. However, at stations far from freshwater inflow areas, brine is in equilibrium with precipitated evaporites, and redox processes (such as sulphate reduction) coupled with secondary sulphide precipitation and brine–evaporite reactions control the dissolved As concentrations. The results confirm that evaporation plays

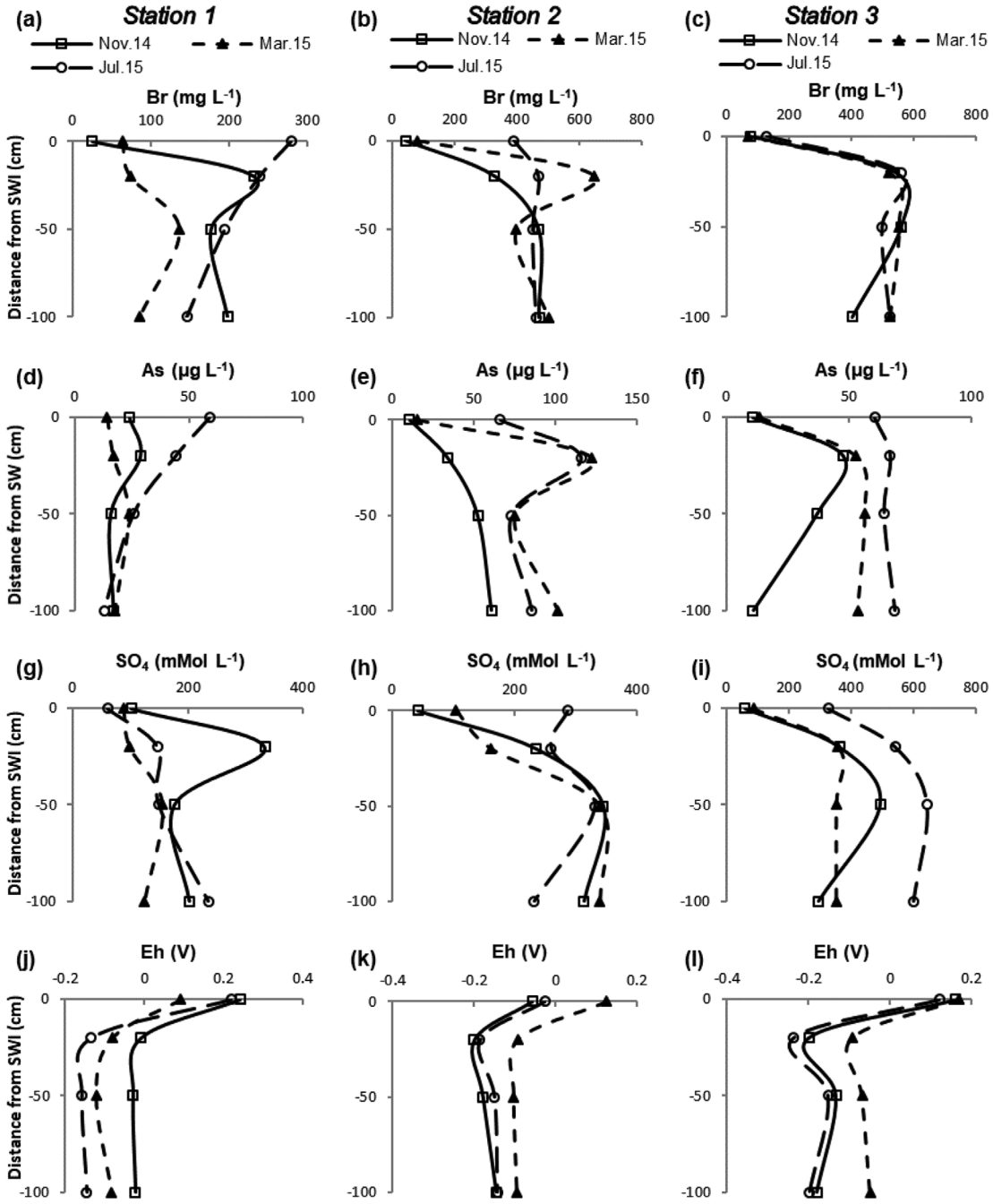

Fig. 11. Vertical profiles (in terms of distance from the sediment–water interface (SWI)) of the (a), (b), and (c) dissolved Br concentrations, (d), (e), and (f) dissolved As concentrations, (g), (h), and (i) dissolved sulphate concentrations, and (j), (k), and (l) redox potentials (Eh values) at stations 1, 2, and 3.

an important role in enriching As in lakes in arid and semiarid areas. The behavior of As in lake sediment PW depends on the redox conditions (and therefore on the content of reactive organic matter, which drives sulphate reduction) and on the sequestration of As and Fe into sulphide minerals.

Acknowledgement

This research was partly financially supported by the Iran National Science Foundation (grant number 96000717). We thank associate editor Huaming Guo and two anonymous reviewers for comments which helped to improve our manuscript.

Appendix A. Supplementary data

Supplementary data to this article can be found online at https://doi.org/10.1016/j.apgeochem.2019.01.008.

References

Alishvandi, B., Fakhire, A., Moghadamnia, A., Samiei, M., 2011. Basic flow separation from direct runoff on the hydrograph of Babahaji River, Maharlu Basin. Seventh Natl. Conf. Watershed Manag. Sci. Eng.

APHA, 1998. Standard Methods for the Examination of Water and Wastewater, twentieth ed. American Public Health Association, Washington, D.C.

Appelo, C.A.J., Postma, D., 2005. Geochemistry Groundwater and Pollution, second ed. A.A. Balkema Publishers, pp. 649.

Bahmani, F., 2009. Hydrogeological relationships and Ion migration of Maharlu Lake adjacent aquifers. In: Geol. Sci. Msc. Thesis. Shiraz University.

Baviskar, S., Choudhury, R., Mahanta, C., 2015. Dissolved and solid-phase arsenic fate in an arsenic-enriched aquifer in the river Brahmaputra alluvial plain. Environ. Monit. Assess. 187. https://doi.org/10.1007/s10661-015-4277-0.
Berner, R.A., 1970. Sedimentary pyrite formation. Am. J. Sci. 268, 1–23.
Bose, P., Sharma, A., 2002. Role of iron in controlling speciation and mobilization of arsenic in subsurface environment. Water Res. 36, 4916–4926.
Brandenberger, J., Louchouarn, P., Herbert, B., Tissot, P., 2004. Geochemical and hydrodynamic controls on arsenic and trace metal cycling in a seasonally stratified US sub-tropical reservoir. Appl. Geochem. 19, 1601–1623. https://doi.org/10.1016/j.apgeochem.2004.02.006.
Cartwright, I., Weaver, T.R., Fiefield, L.K., 2006. Cl/Br ratios and environmental isotopes as indicators of recharge variability and groundwater flow: an example from the souteast Murray Basin, Australia. Chem. Geol. 231, 38–56.
Couture, R.-M., Gobeil, C., Tessier, A., 2010. Arsenic, iron and sulfur co-diagenesis in lake sediments. Geochem. Cosmochim. Acta 74, 1238–1255.
Davis, N.S., Whittemore, D.O., Fabryka-Martin, J., 1998. Uses of chloride/bromide ratios in studies of potable water. Gr. Water 36 (2), 338–350.
Dean Jr., W.E., 1974. Determination of carbonate and organic matter in calcareous sediments and sedimentary rocks by loss on ignition: comparison with other methods. J. Sediment. Res. 44.
Deng, T., Wu, Y., Yu, X., Guo, Y., Chen, Y.W., Belzile, N., 2014. Seasonal variations of arsenic at the sediment-water interface of Poyang Lake, China. Appl. Geochem. 47, 170–176. https://doi.org/10.1016/j.apgeochem.2014.06.002.
Du Laign, G., Chapagain, S.K., Dewispelaere, M., Meers, E., Kazama, F., Tack, F.M.G., Rinklebe, J., Verloo, M.G., 2009. Presence and mobility of arsenic in estuarian wetland soils of the Scheldt estuary (Belgium). J. Environ. Monit. 11, 873–881.
Eugster, H.P., 1980. Geochemistry of evaporitic lacustrine deposits. Annu. Rev. Earth Planet Sci. 8, 35–63.
Eugster, H.P., Jones, B.F., 1979. Behavior of major solutes during closed-basin brine evolution. Am. J. Sci. 279, 609–631.
Fan, L., Zhao, F., Liu, J., Frost, R.L., 2018. The as behavior of natural arsenical-containing colloidal ferric oxyhydroxide reacted with sulfate reducing bacteria. Chem. Eng. J. 332, 183–191.
Farjadian, S., 2006. An investigation on the effect of Maharloo salt lake on the salinity of its north-west adjacent aquifer. In: Geol. Sci. Msc. Thesis. Shiraz University.
Ford, R.G., Wilkin, R.T., Paul, C.J., Beck, F., Lee, T., Scheckel, K.G., Clark, P., 2005. Field Study of the Fate of Arsenic, Lead, and Zinc at the Ground-Water/surface-Water Interface.
Galloway, J.M., Swindles, G.T., Jamieson, H.E., Palmer, M., Parsons, M.B., Sanei, H., Macumber, A.L., Patterson, R.T., Falck, H., 2018. Organic matter control on the distribution of arsenic in lake sediments impacted by ~ 65 years of gold ore processing in subarctic Canada. Sci. Total Environ. 622–623, 1668–1679.
Gao, S., Ryu, J., Tanji, K.K., Herbel, M.J., 2007. Arsenic speciation and accumulation in evapoconcentrating waters of agricultural evaporation basins. Chemosphere 67, 862–871. https://doi.org/10.1016/j.chemosphere.2006.11.027.
Garcia, C.M., Niell, F.X., 1993. Seasonal change in a saline temporary lake (Fuente-De-Piedra, southern Spain). Hydrobiologia 267, 211–223. https://doi.org/10.1007/bf00018803.
Hacini, M., Oelkers, E.H., 2011. Geochemistry and behavior of trace elements during the complete evaporation of the merouane chott ephemeral lake: southeast Algeria. Aquat. Geochem. 17, 51–70. https://doi.org/10.1007/s10498-010-9106-z.
Hammer, U.T., 1986. Saline Lake Ecosystems of the World. Springer Science & Business Media.
Hardie, L.A., 1984. Evaporites; marine or non-marine? Am. J. Sci. 284, 193–240.
Hollibaugh, J.T., Carini, S., Gürleyük, H., Jellison, R., Joye, S.B., LeCleir, G., Meile, C., Vasquez, L., Wallschläger, D., 2005. Arsenic speciation in Mono Lake, California: response to seasonal stratification and anoxia. Geochem. Cosmochim. Acta 69, 1925–1937. https://doi.org/10.1016/j.gca.2004.10.011.
Jia, Y., Guo, H., Xi, B., Jiang, Y., Zhang, Z., Yuan, R., Yi, W., Xue, X., 2017. Sources of groundwater salinity and potential impact on arsenic mobility in the western Hetao Basin, Inner Mogolia. Sci. Total Environ. 601–602, 691–702.
Khosravi, R., 2018. Distribution of arsenic in surface/subsurface water interface of hypersaline lakes. In: Case Study: Maharlu Lake, Fars Province, PhD. Dissertation. Shiraz University.
Khosravi, R., Zarei, M., Bigalke, M., 2018. Characterizing the major controls on spatial and seasonal variations in chemical composition of surface and pore brine of Maharlu Lake, southern Iran. Aquat. Geochem. 24, 27–54.
Kulp, T.R., Hoeft, S.E., Miller, L.G., Saltikov, C., Murphy, J.N., Han, S., Lanoil, B., Oremland, R.S., 2006. Dissimilatory arsenate and sulfate reduction in sediments of two hypersaline, arsenic-rich soda lakes: mono and Searles Lakes, California. Appl. Environ. Microbiol. 72, 6514–6526. https://doi.org/10.1128/AEM.01066-06.
Langner, P., Mikutta, C., Kretzscmar, R., 2012. Arsenic equestration by organic sulphur in peat. Nat. Geosci. 5, 66–73.
Langner, P., Mikutta, C., Kretzschmar, R., 2014. Oxidation of organosulfur-coordinated arsenic and realgar in peat: implications for the fate of arsenic. Environ. Sci. Tecnol. 48, 2281–2289.
Lawson, M., Polya, D.A., Boyce, A.J., Bryant, C., Ballentine, C.J., 2016. Tracing organic matter composition and distribution and its role on arsenic release in shallow Cambodian groundwater. Geochim. Cosmocim. Acta 178, 160–177.
Lyons, W.B., Lebo, M.E., 1996. Observations on the diagenetic behaviour of arsenic in a saline lake: pyramid Lake, Nevada. Int. J. Salt Lake Res. 5, 329–335. https://doi.org/10.1007/BF01995385.
Martin, A.J., Pedersen, T.F., 2002. Seasonal and interannual mobility of arsenic in a lake impacted by metal mining. Environ. Sci. Technol. 36, 1516–1523. https://doi.org/10.1021/es0108537.
McArthur, J.M., Sikdar, P.K., Hoque, M.A., Ghosal, U., 2012. Wate-water impacts on groundwater: Cl/Br ratios for arsenic pollution of groundwater in the Bengal Basin and Red River Basin. Vietnam, Sci. Tot. Environ. 437, 390–402.
McCaffrey, M. a, Lazar, B., Holland, H.D., 1987. The evaporation path of seawater and the coprecipitation of Br- and K+ with halite. J. Sediment. Petrol. 57, 928–938. https://doi.org/10.1306/212f8cab-2b24-11d7-8648000102c1865d.
Moore, F., Forghani, G., Qishlaqi, A., 2009. Surface sediments of the Maharlu Saline Lake, SW Iran. 33.
Najmodini, H., 2011. Investigation of Temporal and Spatial Variations of Heavy Metals in Maharlou Lake and One of Adjacent Aquifers. Msc. Thesis. Shiraz University.
Neubauer, E., von der Krammer, F., Knorr, K.-H., Peiffer, S., Reichert, M., Hofman, T., 2013. Colloidal-associated export of arsenic in stream water during stormflow events. Chem. Geol. 352, 81–91.
Ong, C.G., Herbel, M.J., Dahlgren, R.A., Tanji, K.K., 1997. Trace element (Se, as, Mo, B) contamination of evaporites in hypersaline agricultural evaporation ponds. Environ. Sci. Technol. 31 (3), 831–836. https://doi.org/10.1021/es960531g.
Oren, A., 1999. Bioenergetic aspects of halophilism. Microbiol. Mol. Biol. Rev. 63, 334–348.
Pansu, M., Gautheyrou, J., 2007. Handbook of Soil Analysis: Mineralogical, Organic and Inorganic Methods. Springer Science & Business Media.
Parkhurst, D.L., Appelo, C.A.J., 2013. Description of input and examples for PHREEQC version 3 — a computer program for speciation , batch-reaction , one-dimensional transport , and inverse geochemical calculations. U.S. Geological survey techniques and methods, book 6, chapter A43, 497 p. U.S. Geol. Surv. Tech. Methods, B. 6https://doi.org/10.1016/0029-6554(94)90020-5. chapter A43 6, 6–43A.
Pitzer, K.S., 1987. A thermodynamic model for aqueous solutions of liquid-like density. Rev. Mineral. Geochem. 17, 97–142.
Qishlaqi, A., Moore, F., Forghani, G., 2008. Impact of untreated wastewater irrigation on soils and crops in Shiraz suburban area, SW Iran. Environ. Monit. Assess. 141, 257–273.
Ryu, J.H., Gao, S., Dahlgren, R.A., Zierenberg, R.A., 2002. Arsenic distribution, speciation and solubility in shallow groundwater of Owens Dry Lake, California. Geochem. Cosmochim. Acta 66, 2981–2994. https://doi.org/10.1016/S0016-7037(02)00897-9.
Ryu, J.H., Gao, S., Tanji, K.K., 2010. Speciation and behavior of arsenic in evaporation basins, California, USA. Environ. Earth Sci. 61, 1599–1612. https://doi.org/10.1007/s12665-010-0473-y.
Salati, S., Moore, F., 2010. Assessment of heavy metal concentration in the Khoshk River water and sediment, Shiraz, Southwest Iran. Environ. Monit. Assess. 164, 677–689.
Shakeri, A., Moore, F., 2010. The impact of an industrial complex on freshly deposited sediments, Chener Rahdar river case study, Shiraz, Iran. Environ. Monit. Assess. 169 (1-4), 321–334.
Shariati Bidar, M., 2001. Investigation and Exploration of Economic Elements of the Maharlou, Bakhtegan, Tashk Lakes, Part 1. Geological Survey of Iran, pp. 223 (in Farsi).
Sracek, O., Bhattacharya, P., Jacks, G., Gustafsson, J.P., von Brömssen, M., 2004. Behavior of arsenic and geochemical modeling of arsenic enrichment in aqueous environments. Appl. Geochem. 19 (2), 169–180.
Sracek, O., Berg, M., Müller, B., 2018. Redox buffering and de-coupling of arsenic and iron in reducing aquifers across the Red River Delta, Vietnam, and conceptual model of de-coupling processes. Environ. Sci. Pollut. Control Ser. 25 (16), 15954–15961.
Vega, M., Pardo, R., Barrado, E., Debán, L., 1998. Assessment of seasonal and polluting effects on the quality of river water by exploratory data analysis. Water Res. 32, 3581–3592. https://doi.org/10.1016/S0043-1354(98)00138-9.
von Brömssen, M., Jakariya, M., Bhattacharya, P., Ahmed, K.M., Hasan, M.A., Sracek, O., Jonsson, L., Lundell, L., Jacks, G., 2007. Targeting low-arsenic aquifers in matlab upazila, southeastern Bangladesh. Sci. Total Environ. 379, 121–132.
Welch, A.H., Lico, M.S., 1998. Factors controlling As and U in shallow ground water, southern Carson Desert, Nevada. Appl. Geochem. 13, 521–539. https://doi.org/10.1016/S0883-2927(97)00083-8.
Wilkin, R.T., Ford, R., 2006. Arsenic solid-phase partitioning in reducing sediments of a contaminated wetland. Chem. Geol. 228, 156–174. https://doi.org/10.1016/j.chemgeo.2005.11.022.
Zabala, M.E., Manzano, M., Vives, L., 2016. Assessment of processes controlling the regional distribution of fluoride and arsenic in groundwater of the Pampeano Aquifer in the Del Azul Creek basin (Argentina). J. Hydrol 541, 1067–1087. https://doi.org/10.1016/j.jhydrol.2016.08.023.
Zak, I., Gat, J.R., 1975. Saline waters and residual brines in the Shiraz-Sarvistan basin, Iran. Chem. Geol. 16, 179–188.